JOINT INSTITUTE FOR NUCLEAR RESEARCH, DUBNA
Report 10 - 7617

AUTOMATIC GAIN CONTROL IN THE SIGNAL-PROCESSING CIRCUIT OF THE SPIRAL READER

K. Wattenbach, V.M. Kotov, R. Poze, A.E. Selivanov

Dubna 1973

Translated at CERN by R. Luther
(Original: Russian)
Not revised by the Translation Service

(CERN Trans. Int. 75-1)

Geneva
August 1975

INTRODUCTION

When bubble-chamber pictures are processed automatically, variations in the film transparency in the frame area may cause difficulties. However, the spatial reconstruction of particle tracks calls for a great deal of accuracy when measuring the co-ordinates of points on the tracks. Therefore, automatic devices for measuring chamber pictures must be designed in such a way that the signal-processing circuit eliminates the effect of variations in background.

During the development of the Spiral Reader at Dubna, a proposal was made for a variant of method /1/ which is based on dark bubble images on a light background (a variant based on light bubble images on a dark background was also studied).

In the Spiral Reader the position of the bubbles on the tracks is measured in polar coordinates, and radius R changes more than 100 times during the measurement process. This means that the transmission curve of the signal gain channel must vary according to the scanning radius : at same time the width of the pass band must not change. Only in this way can an approximately constant signal-to-noise ratio be achieved throughout the range of variation R.

PRINCIPLES OF OPERATION

The photomultiplier's anode current may easily be varied over a wide range (two orders of magnitude) if the voltage between the anode and the last dynode is changed whilst the supply voltage U_{ak} and the illumination of the photocathode remain constant, and if the anode current is measured by an instrument with a low internal resistance. Fig. 1 shows the dependence of the anode current on the anode-dynode voltage for certain photomultipliers. The measurements were carried out under the conditions shown. The plots indicate some saturation in the region of negative voltages on the dynode. This means that all the secondary electrons emitted by the last dynode reach the anode. When the dynode's potential is increased, some of the secondary electrons are held near it, thus producing a space charge. The number of electrons which reach the anode from the space charge cloud depends on the value and sign of the voltage between the anode and dynode. Moreover, the space charge also helps to make the signal-to-noise ratio higher in the anode current than in the cathode current. Consequently, when one is dealing with a light flux which is modulated in the direction of its attenuation, the photomultiplier should operate in the space-charge mode : when the light is pulse-modulated, this mode is less convenient. Fig. 1 also shows that the control voltages lie within the effective range of integrated operational amplifiers.

There is a noticeable difference in the characteristics curve $I_a = f\ (U_q)$ of the EMI 9656A photomultiplier (viz fig. 1) and the two other types of photomultiplier : this is due to differences in design. Since the EMI 9656A is a venetian blind multiplier, the rate of rise of its output signal is much higher than that required for the Spiral Reader and similar instruments. It is therefore a very convenient light-sensitive component for such instruments.

BLOCK DIAGRAM OF ANODE CURRENT STABILIZATION

If the multiplier's anode current is fed to an amplifier with negative feed-back A1 (fig. 3), a voltage proportional to that current is produced at the amplifier's output. If the output voltage is compared to the reference voltage in comparison circuit A2 and the output voltage of A2, which is proportional to the difference between the input voltages, is transmitted directly to the last dynode, then it will vary in such a way that the anode current I_a remains constant and equals the value set by the reference voltage.

If amplifier A1 has a large width (transmission curve B, fig. 3) and amplifier A2 has a narrower pass band (curve C), then the pass band for the whole circuit will correspond to curve D, i.e. by selecting the appropriate transmission curve for amplifier A2, it is possible to suppress the undesirable low-frequency component in signal current I_a.

OPTIMIZATION OF THE SIGNAL-TO-NOISE RATIO

The noise voltage at the output of amplifier A1 consists of two components : noise from the multiplier and the amplifier's own noise. Of course, the higher the signal-to-noise ratio in the output voltage U_A (fig. 4), the better the measurement accuracy. The signal-to-noise ratio in the multiplier's anode current I_a is directly related to the light flux incident on the photocathode. A strong effect is also exerted by the length of the light flux wave which determines the quantum yield. A high quantum yield is obtained when a SbKNaCs photocathode is used. The maximum quantum yield and the minimum noise coincide. Fig. 2 shows the wave-length dependence of the relative energy distribution of an incandescent tube and a In J-filled gas discharge tube, and also the relative wave-length dependence of the quantum yield and noise voltage of a FEU-68 multiplier.

A rough estimate shows that an incandescent tube requires approximately ten times as much luminosity in order to obtain the same signal-to-noise ratio as in a gas discharge tube. The signal-to-noise ratio is also affected by the quality of the electron optics between the cathode and the first dynode : this quality substantially depends on the voltage between the cathode and the dynode. It is therefore recommended to stabilize this voltage /3/.

Consequently, the photomultiplier's signal-to-noise ratio is determined by the given optical system since the gain and hence the anode current may be increased by raising the supply voltage. However, this does not improve the signal-to-noise ratio since the mean distribution of electrons emerging from the photocathode during the multiplication process does not change. The photomultiplier is an ideal wide-band amplifier because the product of the amplification factor times the band width increases with the gain. On the other hand, in the case of a conventional amplifier the product of the amplification factor times the band width is a constant, and the band width may be increased only be reducing the amplification factor and vice-versa. Consequently, the signal-to-noise ratio may be improved only by improving the optical system or by increasing the luminosity of the light source.

The noise voltage of a bipolar silicon transistor in a circuit with a common emitter depends on two values /4/, i.e. the emitter current and the internal resistance of the signal source. The minimum noise voltage values occur in the region of low, 20-30 μA, emitter currents and when the internal resistance of the signal source is approximately 10-30 k Ohm. This requirement corresponds to the mode of the input stage of the IUT402 operational amplifier.

The emitter current of the input cascade of an integrated operational amplifier may be varied within certain limits by changing the supply voltage.

Contemporary types of integrated amplifier with so-called super beta transistors have correspondingly small currents at the working points.

DESCRIPTION OF THE COMPLETE CIRCUITS

As stated above, the film information consists of a dark bubble image on a light background. Therefore, the photomultiplier is always illuminated, and the light flux decreases only when a bubble image passes. For this mode of operation, the photomultiplier's maximum anode current specified by the manufacturer is I_a max = 50μA. Assuming that the background density changes 100 times, the anode current will vary from 50 to 0.5 μA outside the bubble image. Current I_a is supplemented by the variation in the anode current I_a caused by the bubble image. The light modulation caused by the bubble image in light or dark surroundings may be considered the same to a first approximation /5/.

The basic AGC circuit is shown in fig. 4. The operation of the circuit may be described as follows :
if, for instance, current I_a is reduced at the input of amplifier A1, this causes an unbalance at the input of comparison circuit A2, at the output of which a maximum negative voltage is set up. The current from the last dynode increases and is completely absorbed by the anode, thus compensating the unbalance until there is no difference in the input voltages at A2. The closed control circuit begins to operate, and the anode current assumes its former value. If the multiplier's gain is increased by the increase in the supply voltage or if the anode current is increased by the increase in the light flux, then these changes are absorbed by the space charge of the last dynode. The dynode's maximum direct current of 50 μA is the upper limit in this case. Consequently, not only the fluctuations in the anode current but also the drift of amplifier A1 are compensated. (E.g. heat drift, time drift etc.). The oscillations occurring in the pass band of amplifier A2 are compensated. All components with high frequencies, which include the signal, are not balanced.

The end of the pass band of amplifier A2 (plot C in fig. 3) and the beginning of the signal band must be far enough apart for the multiplier to operate with a constant voltage on the dynode during the passage of the signal from the bubble. A C-type transmission curve (viz. fig. 3) is produced by triggering a peak detector after amplifier A2. The storage capacitor of this peak detector is discharged by a current proportional to the radius. A variable upper limit of band A2 is thus produced which determines the optimum filtration of the signal's lower limit. The filtration of interference with higher frequencies than those contained in the signal is achieved by a filter amplifier with a variable cut-off frequency which is located outside the closed control circuit and is not described here.

Amplifier A2 operates constantly outside the linear region because the noise voltage at output A1 is higher than the control region of A2 (fig. 6). Therefore the frequency response curve of amplifier A2 is not important. It operates like a rectifier and does not affect the stability of the control circuit.

The peak detector's capacitor is charged to the maximum positive noise voltage. However, this depends on the density of the pulses in the noise signal. The transient process in the AGC circuit after the jump from light to dark has affected the photomultiplier is determined only by amplifier A1. If the signal does not return to its initial level, the dynode voltage is reduced with the peak detector's time constant until the initial level is restored at the A1 output. The gain control circuit then follows the background variations again. The disadvantage of the peak detector circuit is that the capacitor's discharge current, which varies as the radius increases, affects the level of the output voltage and that this variation occurs at the very end of the control circuit. The emitter follower formed by the transistor T2 reduces this effect 20-30 times.

STABILITY OF THE AUTOMATIC GAIN CONTROL CIRCUIT

As stated in the previous section, the transient response and stability of the AGC circuit are mainly determined by the parameters of amplifier A1.

Operational amplifier 1UT402 (A1) has no internal frequency compensation and therefore when it is used with negative feed-back correcting circuits are required to suppress oscillations at the upper frequency limit. The correcting circuits offered by the manufacturer did not allow the output voltage to be varied at the fast rate required for the Spiral Reader. It was necessary to change the correcting circuits so that they guaranteed the stability of the circuit and at the same time increased the rate of variation of the output voltage by one order of magnitude. The feed-back stage affects the choice of time constant for the correcting circuits.

The RC circuits were matched experimentally by increasing the rate of variation of the output voltage approximately 20 times whilst the AGC circuit was in stable operation. However, the compensation is not calculated for the worst cases, and it is therefore necessary to investigate its transient process after excitation of the amplifier by a step function.

RESULTS OF THE TESTS

In order to check the reliability of the proposed AGC circuit, tests were carried out and the circuit's characteristics measured on a special bench where a 100-fold variation in the illumination of the photocathode could be simulated and the light varied over the necessary amplitude and frequency range.

The plots (fig. 5) show that, for an output signal height of 1.5-3V, which is quite adequate for the subsequent signal processing circuits, a variation of two orders of magnitude in the illumination of the multiplier is compensated by the AGC circuit which still retains a considerable reserve of control.

The new correction loops for the operational amplifier IUT402 (A1) allow a rate of rise of the output signal of 2V/μsec.

Fig. 6 shows oscillograms of the video signals at the AGC reference points.

Bibliography

1. Rosenthal, Jerome A. and Fiehrer M. Automatic Gain Control for Photomultiplier Tubes. The Review of Scientific Instruments Vol. 35 (1964) No. 11S. 1560.
2. A.Ya. Astakhov et al. JINR Report, RIO-4943, Dubna, 1970.
3. Photomultiplier Tubes. EMI Electronics Ltd. Electron Tube Division Hayes Middlesex G.B.=
4. H.P. Walker. Low-Noise Audio Amplifiers. Wireless-World Vol.78.
5. G. Fontaine, G. Reboul. Automatic Gain Control in Signal Processing for Bubble Chamber Pictures. International Conference on Data Handling Systems in High-Energy Physics. Lord D.H. Powel B.W. CERN 70-21 Vol 1 S. 383.
6. A.V. Pavlov, A.I. Chernikov. Detectors for automatic optico-electronic instruments "Energiya", Moscow, 1972.
7. Use the Two-Stage RC-Low-Pass-Filter as Approximation for Matched Filters. Electronic Design. Vol. 19 No. 26 (dec. 23 1973) Design Ideas.
8. S. Reynand, E. Rossa. Controle automatique de gain et normalization des impulsions de sortie sur le lecteur en spirale digitisee LSD. Preprint CERN Inst. 71-5.
9. K. Larche. Moderne Gluh-und Entladungslampen (Indium Iodid Entladungslampen). Die Naturwissenschaften 56 (1969) No. 9, S. 429-434.

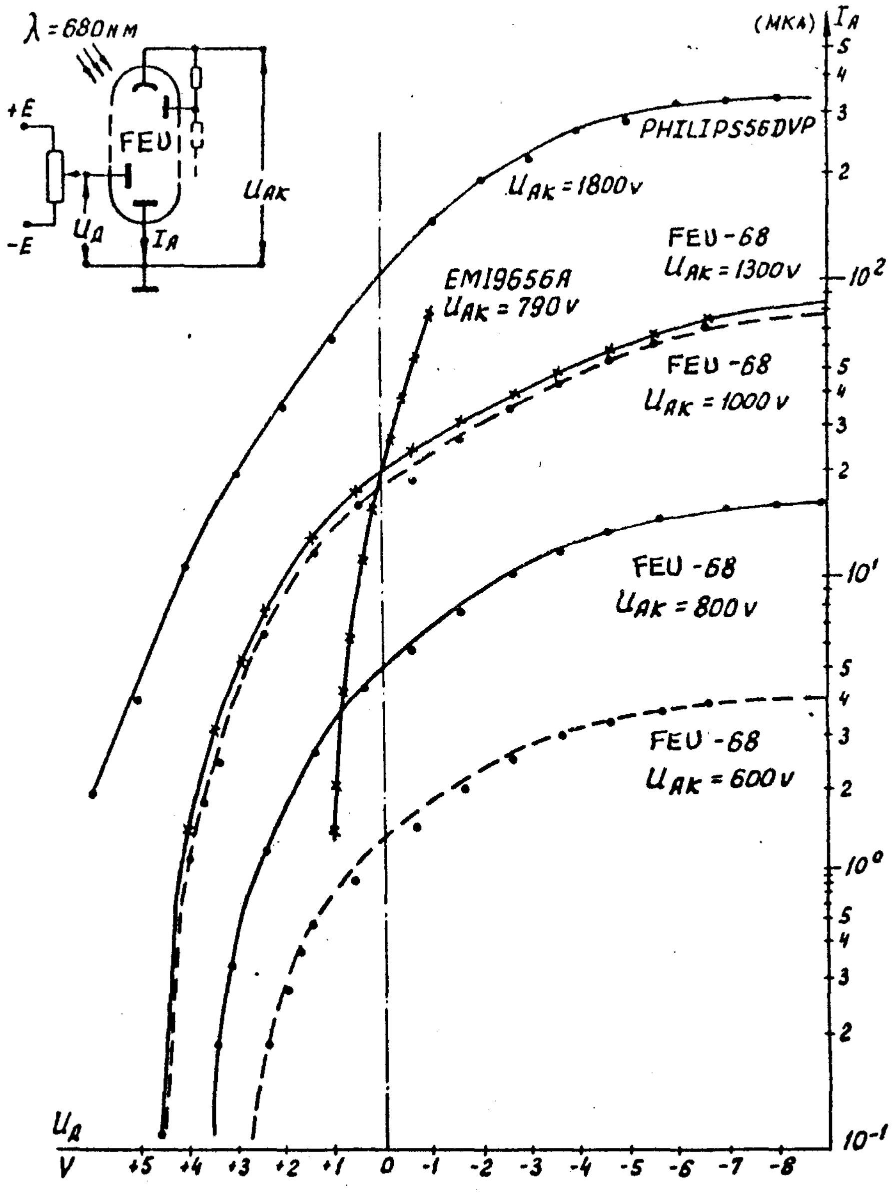

Fig. 1 FEU = photomultiplier

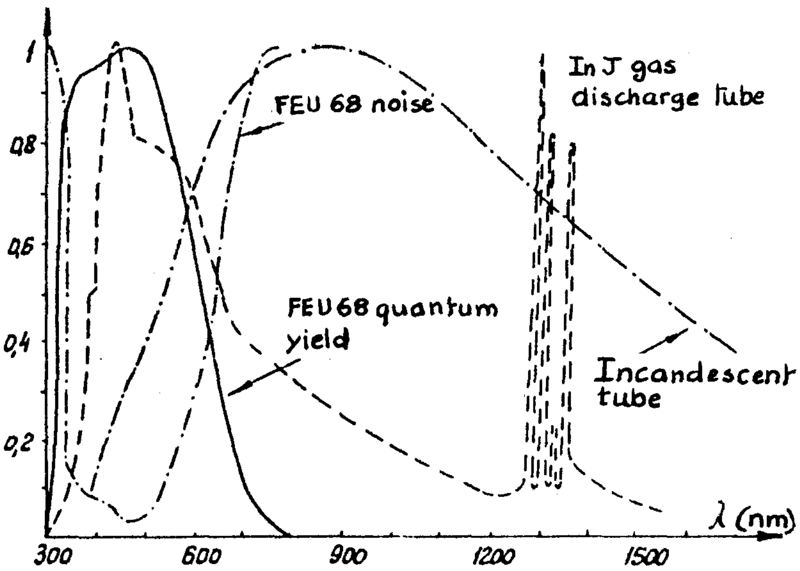

1
0,8
0,6
0,4
0,2
300
600
900
1200
1500
λ (nm)
FEU 68 noise
In J gas
discharge tube
FEU 68 quantum
yield
Incandescent
tube

Fig. 2

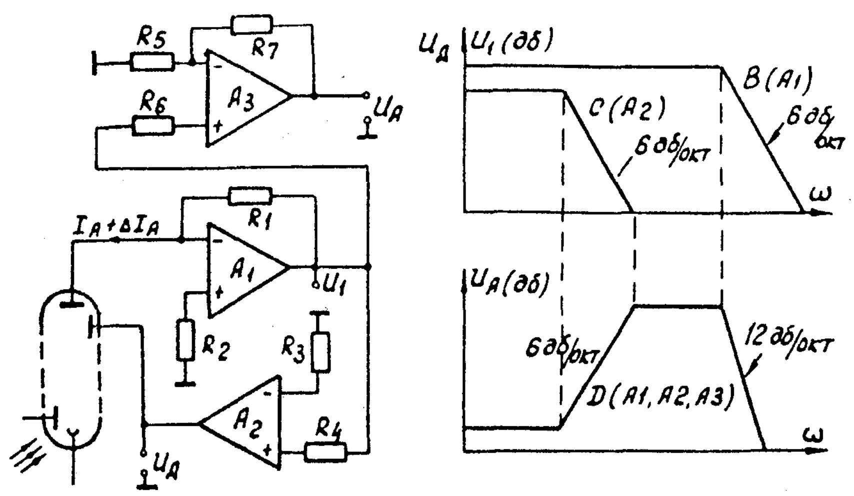
R5
R7
A3
R6
UA
R1
IA+ΔIA
A1
U1
R2
R3
A2
R4
UA
UA
U1(дб)
C(A2)
B(A1)
6дб/окт
6дб/окт
ω
UA(дб)
6дб/окт
12дб/окт
D(A1, A2, A3)
ω

Fig. 3

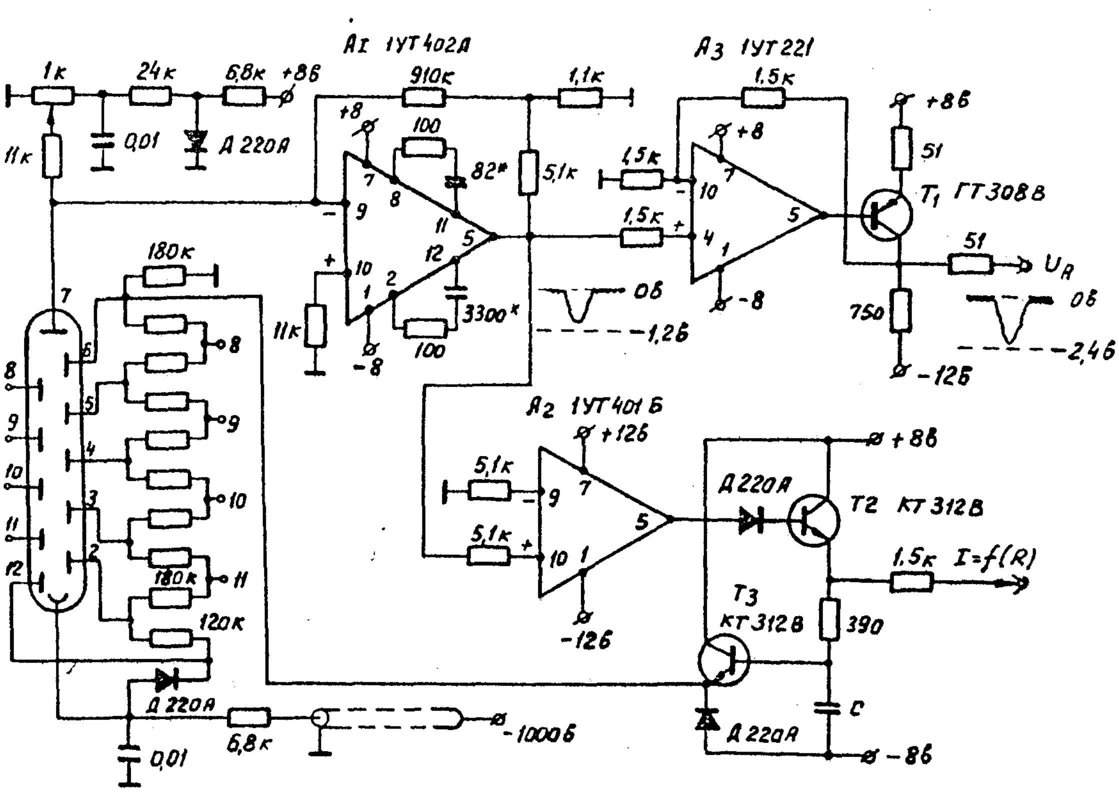

AI 1УТ402А
A3 1УТ221
A2 1УТ401Б
1к
24к
6,8к +8в
0,01
Д220А
11к
910к
1,1к
100
82*
5,1к
1,5к
3300*
180к
120к
T1 ГТ308В
51
750
UR
0в
-1,2в
-2,4в
-12Б
+8в
-12в
+12в
T2 КТ312В
T3 КТ312В
390
I=f(R)
C
-8в
-1000в
6,8к

Fig. 4

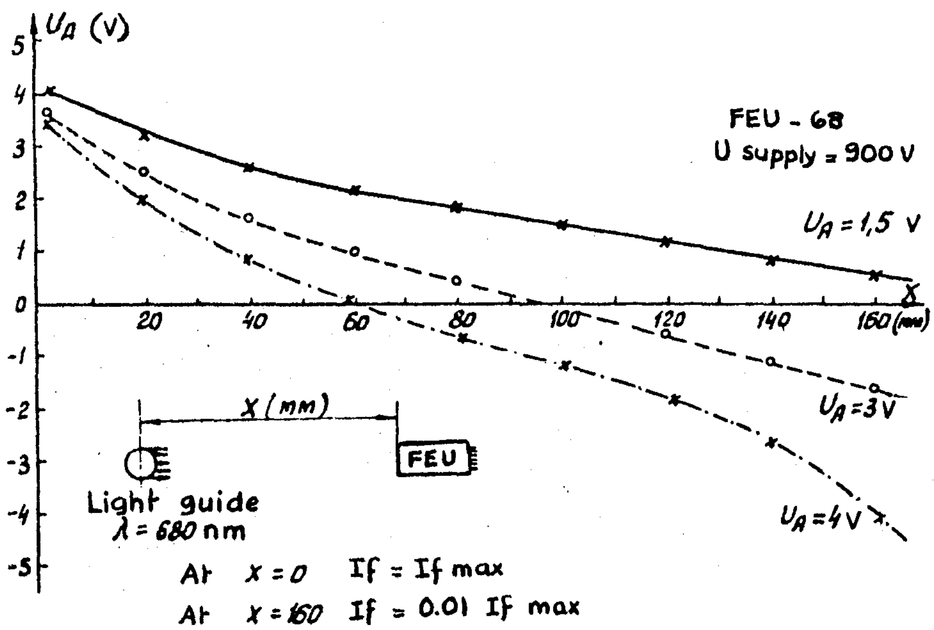

U_A (V)
5
4
3
2
1
0
-1
-2
-3
-4
-5
20
40
60
80
100
120
140
160 (mm)
X
FEU - 68
U supply = 900 V
U_A = 1,5 V
U_A = 3 V
U_A = 4 V
X (mm)
FEU
Light guide
λ = 680 nm
At X = 0 If = If max
At X = 160 If = 0.01 If max

Fig. 5

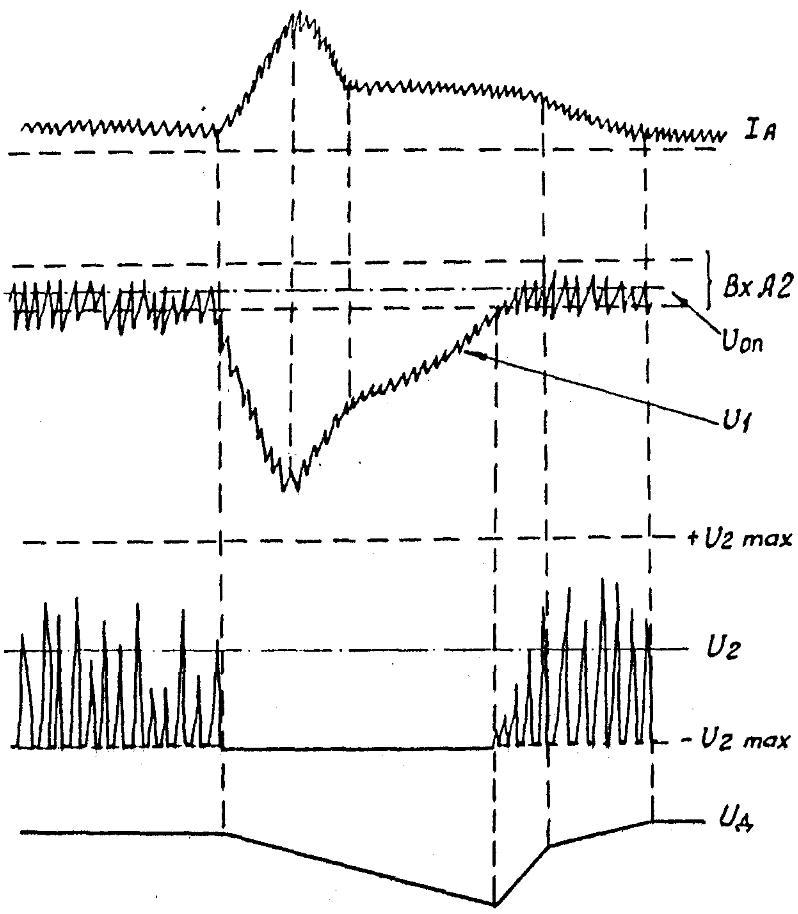

Fig. 6